HIGH FREQUENCY PARAMETRIC EVALUATION AND STRUCTURAL ANALYSIS OF DISCRETE COMPONENTS IN A PRINTED CIRCUIT BOARD

Pearson.T[1], Madheswaran.M[2]
[1]SMK Fomra Institute of Technoilogy, Chennai, India.
[2]Muthayammal Engineering College, Rasipuram, India.
Email: [1]pearsonin@gmail.com

Abstract:

There can be various EMC expert systems developed for analyzing the PCB. The algorithms used to predict possible radiated emissions problems from a printed circuit board have been presented. From accuracy point of view, the expert system approach is approximately equal to human EMC expert with a through knowledge of the board and a calculating aid. The algorithms also make assumptions and approximations about how the board will interact with the rest of the system.

Keywords: EMI, EMC, EMS, Standards, Expert System.

I. INTRODUCTION

Electromagnetic compatibility (EMC) often refers to one of the mysteries in the field of electrical and electronic engineering, as the EMC behavior of a product is unpredictable. In most cases, the EMC performance of the product cannot be found precisely with the highest level of simulation tools [1]. No single simulation software covers all the parameters and the rules governing the EMC design. Most of the engineers rely on measurement and testing methods after the prototype of the product is fabricated. In large-scale electrical and electronic projects, the end result may be catastrophic when there are critical EMC problems identified after the completion of infrastructure.

II. The Problem

Following rapid development of science and technology, human society has entered into a new era of information technology and communication in the 21st century. Today, the whole environment is surrounded by the significant levels of background electromagnetic noise emitted from mobile communication networks, computers, microprocessors, electrical appliances and so on. It is estimated that there is a 7% - 14% increase in the background.

The severe electromagnetic noise environment is hazardous towards electrical and electronic equipment, especially valuable electronic control system. The electromagnetic hazard is a cause for great concern around the world. A world-wide study and research are then initiated for electromagnetic noise reduction techniques. Recent research not only concentrates on electromagnetic noise reduction, but also on compatibility between equipment and environment in electromagnetic aspects. Therefore a broader term electromagnetic compatibility (EMC) is referred to, to cover the wider scope. This means that the electrical/electronic equipment is compatible with each others without any deterioration in their function within a defined time and space.

EMC refers to two aspects, electromagnetic interference (EMI) and electromagnetic susceptibility (EMS). EMI refers to the noise level generated by the equipment, which causes interference with others while EMS refers to the immunity of equipment against electromagnetic noise from the environment. Equipment with good electromagnetic compatibility emits minimum noise to the environment as well as being able to resist the noise from the environment. The existence of electromagnetic compatibility requires three conditions:

a) Equipment to generate electromagnetic noise-(source)
b) Equipment to receive electromagnetic interference-(victim)
c) Media for the electromagnetic noise -(comply with)

Their relationship is illustrated in Figure 1.

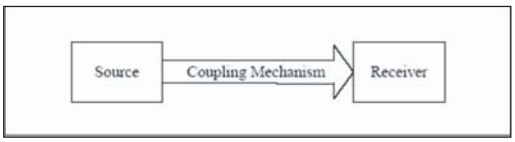

Fig. 1. Basic Elements in EMI Problems

The coupling path is the emission path of the electromagnetic noise. It is equivalent to the transmission of electromagnetic energy. Moreover, it is divided into conducted emission and radiated emission. Conducted emission requires certain transmission media but radiated emission does not require any. Radiated emission is classified into the near field and far field depending on the transmission distance d and the wavelength of the transmission wave λ

III. EXPERT SYSTEM

There can be various EMC expert systems developed for analyzing the PCB. One of the EMC expert system developed for PCB generally consists of four stages as listed below [2].

1. Input
2. Classification
3. Evaluation
4. Reporting

The board layout and component input data, the characteristics of all the net list and their signals are identified in the net classification stage. This information is passed to evaluate algorithms, which search for possible radiation or susceptibility problems. In this, the radiation algorithms, there are five different radiation algorithms as follows.

a. Differential-Mode Radiation algorithm:

This calculates the direct radiation from signal traces.

b. Current-Driven Common-Mode Radiation algorithm:

It determines how best each circuit is able to drive common-mode currents onto the cables or enclosures by way of magnetic field coupling.

c. Voltage-Driven Radiation algorithm:

This focuses on the electric field coupling.

d. I/O coupling algorithm:

This calculates the radiation due to noise coupled directly to trace that conduct energy off the board.

e. Power Bus Radiation algorithm:

The radiation from power-bus structures on high-speed printed circuit boards due to the switching noise current of digital integrated circuits is investigated

IV. STRUCTURE OF THE RADIATION PCB EMC EXPERT SYSTEM

The basic structure of the PCB EMC expert system by using board layout and components input data, the characteristics of all the nets and their signals are identified in the net classification stage. This information is passed to the evaluation algorithms, which search for possible radiation or susceptibility problems[3]. The radiation algorithms in the evaluation stage are, the Differential-mode radiation algorithm, the Current-driven common-mode radiation algorithm, the Voltage-driven radiation algorithm, the Radiation by I/O coupling algorithm and the Power Bus radiation algorithm as illustrated in the figure 2.

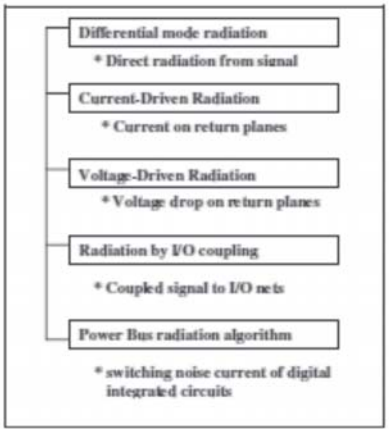

Fig. 2. Radiated Emission Algorithms

V. SYSTEM ANALYSIS OF THE TEST BOARD

A multilayer test board is used to evaluate the expert system algorithms experimentally. This test board shown in figure 3, is developed for a study of the effects of layer spacing and dielectric materials on radiation algorithms. The following diagram in the figure 3 illustrates layer stack up of the test board.

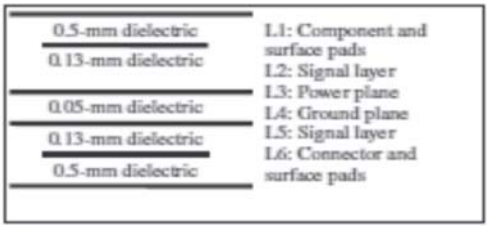

Fig. 3. Layer stack up of the test board

In the test board Power and Ground planes are located on layer 3 and layer 4 with a spacing between them, 0.05 mm. Signals are routed on layer 2 and layer 5. The components consists of one 50-MHz oscillator, one bulk decoupling capacitor, eight octal clock buffers, 28 load capacitors and 32 local decoupling capacitors. A subminiature type-A coaxial connector is used to connect to the power supply 3.3-V power supply.

VI. EXPERT SYSTEM ANALYSIS OF THE TEST BOARD

A. Board Analysis Using the Differential Mode

This algorithm models signal trace segments and their corresponding return trace segments as current loop radiation sources[4].

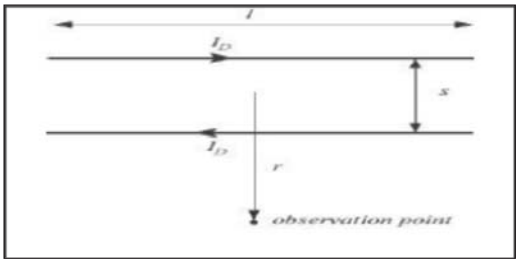

Fig. 4. A simple differential mode current radiation source

The maximum electric filed is given by the formula,

$$|E|max = 1.316 \times 10^{-14} |I_D| f^2 l s / r \quad (1)$$

Where f is the frequency in Hz, l is the length of a segment, s is the distance between trace and return trace, I_D is the magnitude of the return current, r is the-radius of the electric field intensity (generally considered as 3m). Hence simplifying the equation we get,

$$|E|max = 4.4 \times 10^{-15} |I_D| f^2 L d \quad (2)$$

Since most EMI regulations require measurements in a semi-anechoic environment, the electric field[5] is multiplied by a factor of two to account for the worse case of reflection off the floor. Therefore the final equation can be written as,

$$|E|max\ 10^{-14} |I_D| f^2 L d \quad (3)$$

The differential emission estimate for the entire board is obtained by taking a root mean square sum of the fields for each net as,

$$|El_{total} = \sqrt{(E_{net\,1})^2 + (E_{net\,2})^2 + \ldots + (E_{net\,n})^2} \quad (4)$$

The parameters needed to calculate the radiation by the differential mode radiation algorithm are listed in Table 1.

Table 1. Parameters needed Differential mode algorithm

Parameter	Description	Value
L	Board length	7.6 cm
W	Board width	5.0 cm
h	Space between power planes	0.05 mm
ε_r	Dielectric permittivity	3.88
R_s	Average resistance of the components	0.3 ohms
L_s	Average inductance of the components	1.4 nH
t_1	Rise/fall time of the current signal	1.5 ns
t_2	Rise/fall time of the current signal	1.5 ns
T	Period of the signal	20 ns
C_{PL}	Power dissipation capacitance	20 pF/gate

Figure 5 shows that radiated emissions of the PCB in frequency range 300 – 400 MHz have exceeded the CISPR 22 Class B limit marginally.

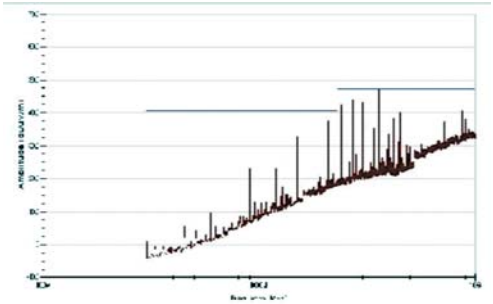

Fig. 5. Radiated emissions for PCB layout

To show the possible impact of CM radiation of the PCB, a 30 cm wire is soldered at the far end PCB ground, directly opposite the 9 V source.

Figure 6 shows the radiated emissions of the PCB with the attached wire. It indicates clearly that the added CM radiation due to the attached wire pushes the emissions up significantly and now the highest emission exceeded the limit by as much as 20 dB.

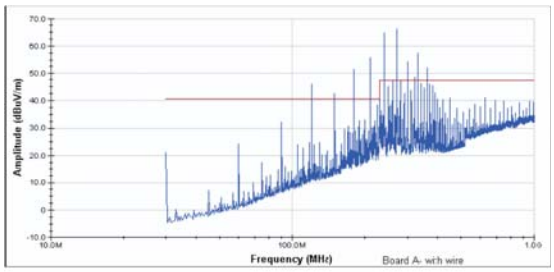

Fig. 6. Radiated emissions for PCB with attached wire

The high CM radiation is due to the large ground bounce on the PCB ground resulting from poor layout. The high frequency parametric and structural analysis of the Differential Mode Radiation Algorithm for the test board is illustrated in the figure 7 and 8.

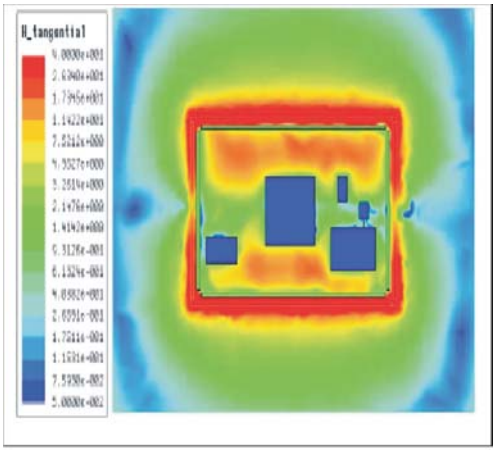

Fig. 7. High frequency parametric and structural analysis of the H-field in Differential Mode Radiation Algorithm

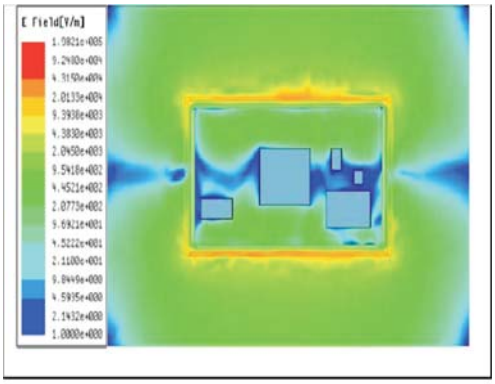

Fig. 8. High frequency parametric and structural analysis of the E-field in Differential Mode Radiation Algorithm

B. Board Analysis Using the Current-Driven Radiation Algorithm

Considering the width of the printed circuit board to be finite, a portion of the magnetic field due to a signal current wraps around the board and there is an effective voltage drop across the return plane as shown in Figure 9. This voltage drop, in turn, can induce common mode currents that drive various EMI antennas on the printed circuit board[6]. These EMI antennas could be cables, heat sinks or other metallic structures.

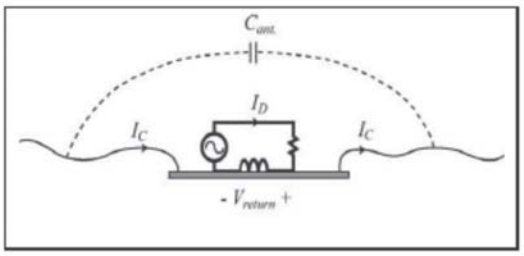

Fig. 9. A simple configuration illustrating current-driven common mode configuration

The expert system estimates the voltage difference by approximating the branch inductance of the current return path as

$$L_p = (4/\pi^2) \times [(\mu_o l\, h)/(dist1 + dist2)] \qquad (5)$$

Where h is the height of the trace over the return plane, dist1 & dist2 are the two shortest distances between boundary of the board from midpoint of the segment, l is the length of a segment and μo is the permeability. The potential difference across the printed circuit board is calculated as

$$V_{ret} = \omega L_p I_{DM} \qquad (6)$$

Where V_{ret} is the return voltage, ω is the angular frequency, L_p is the branch inductance and the IDM is the differential mode current.

For the board under analysis[7], there were no heat sinks, and there was only one cable attached to the board.. The parameters needed to calculate the radiation by the current-driven CM radiation algorithm and their values are listed in Table 2.

Table 2 .Parameters needed for current driven algorithm

Parameter	Description	Value
L	Board length	7.6 cm
W	Board width	5.0 cm
h_i	Height of trace above plane	Depends on individual trace
l_i	Trace length	Depends on individual trace
ε_r	Dielectric permittivity	3.88
$dist1$	Shortest distance to one board edge	Depends on individual trace
$dist2$	Shortest distance to another board edge	Depends on individual trace
Δt	Current pulse width	3 ns
T	Period of the signal	20 ns
C_L	Load capacitance of the signal traces	16 x 7 pF

There were a total of seven signal traces on the second layer of the board contributing to the current-driven common mode radiation. The signal current on each trace was approximated as a triangular pulse with a

pulse width of Δt, a period of T, and a peak value of Ip = $C_L V_{CC}/\Delta t$. Figure 10 shows the envelope of the maximum estimated radiated emissions calculated using the current-driven CM radiation algorithm At low frequencies (e.g., below 300 MHz), the radiation is limited primarily by the ability of the board-cable structure to form an efficient antenna. At higher frequencies, the radiation falls off in proportion to the amount of energy in the source current waveform as illustrated in the figure 10.

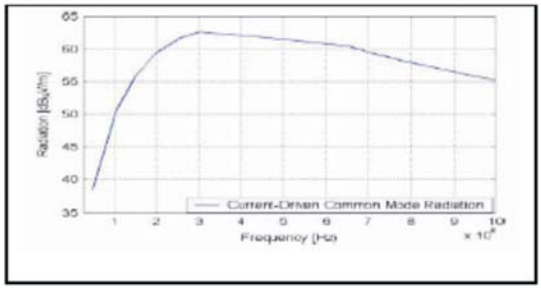

Fig. 10. Maximum emissions calculated using the current-driven common mode radiation algorithm.

The high frequency parametric and structural analysis of the Current-Driven Radiation Algorithm for the test board is illustrated in the figure 11 and 12.

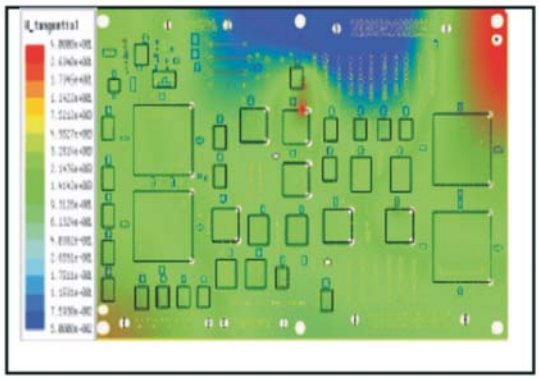

Fig. 11. High frequency parametric and structural analysis of the H-field in Current-Driven Radiation Algorithm

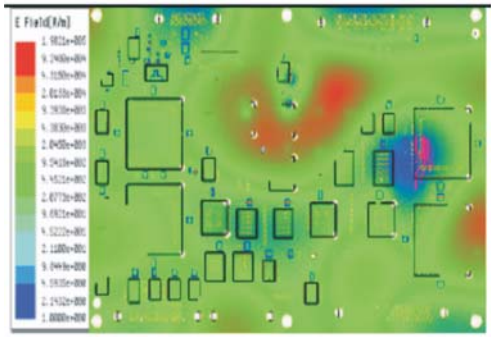

Fig. 12. High frequency parametric and structural analysis of the E-field in Current-Driven Radiation Algorithm

C. Board Analysis Using the Voltage-Driven Radiation Algorithm

Any metallic structures that are at a different potential than other metallic structures may carry common mode currents and, in turn, create radiated emissions.

The following illustration shows Signal or component voltage appears between two good antenna parts.

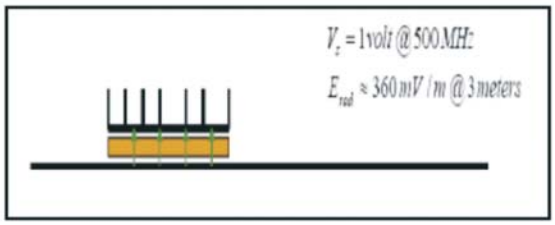

Fig. 13. A simple configuration illustrating voltage-driven common mode configuration

The figure 13 shows it the signal appearing at the device is at 1volt with the frequency 500 MHz, and then the radiated emissions magnitude is approximating to the 360 mV at a distance of 3 meters. Assuming the board is electrically small, the electric fields coupled to the attached cable can be represented by an effective mutual capacitance between the trace and the cable C_{t-c}.

However, the common-mode current flowing on the cable is primarily responsible for the radiated emissions. The conversion from differential-to common-mode can be modeled by placing equivalent common-mode voltage[8] sources at locations where there is a change in the "balance" of the structure. In this case, the dominant effective common-mode source occurs at the junction between the cable and the plane as illustrated in Fig. 14.

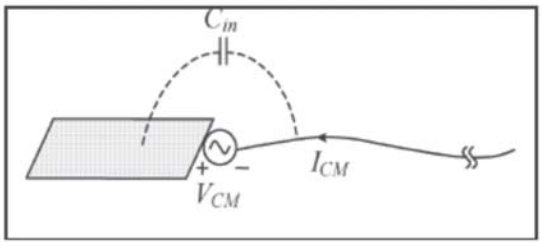

Fig. 14. Equivalent wire antenna model for voltage-driven coupling.

Therefore, the magnitude of the common-mode voltage source can be expressed as

$$V_{CM} = \frac{C_{t-c}}{C_{in}} V_{DM} \qquad (7)$$

Approximating the antenna as an isotropic source, the radiated power is given by

$$P_{rad} \approx \oiint \frac{1}{2}\frac{|E|^2}{\eta_0} ds = \frac{4\pi r^2 |E|^2}{2\eta_0} \equiv \frac{1}{2} I_{CM}^2 R_{rad} \quad (8)$$

where $\eta_0 = 120\pi$, and R_{rad} is the radiation resistance of the antenna. Since, in general, the radiated emissions are measured in a semi-anechoic chamber, the estimated field is multiplied by a factor of 2 to account for the worst-case reflection off the floor. The common mode current can be expressed in terms of an equivalent common mode voltage VCM appearing between the board and the cable. The maximum radiated field is then given by

$$|E|_{max} \approx \frac{2V_{CM}}{r}\sqrt{\frac{30}{R_{rad}}} \approx 1.1\frac{V_{CM}}{r} \quad (9)$$

The voltage-driven algorithm was first applied to the test board for the case where the buffers were not loaded. The common mode voltage and the radiated electric field due to each signal trace were obtained from the following equation

$$|E|_{max} \approx \frac{2V_{CM}}{r}\sqrt{\frac{30}{R_{rad}}} \approx 1.1\frac{V_{CM}}{r} \quad (10)$$

The board parameters used to calculate the radiation are listed in Table 3.

Table 3. Parameters needed for voltage driven algorithm

Parameter	Description	Value
L	Board length	7.6 cm
W	Board width	5.0 cm
h_t	Trace height over power planes	0.625 mm for top layer traces 0.125 mm for second layer traces
l_t	Trace length	Depends on individual trace
a	Trace width	Depends on individual trace
t_r	Rise time of the voltage signal	1 ns
t_f	Fall time of the voltage signal	1 ns
T	Period of the signal	20 ns
τ	Pulse width of the signal	10 ns

In this case, we would expect the voltage-driven emissions to be dominant. There were 28 buffer load mounting pads each with a size of about 2 mm×1.5 mm (four for each buffer) on the top layer of the board. The pads were connected to the buffers through 28 traces, each with a length of about 1 cm and a width of about 0.5 mm, on the second signal layer of the board. Assuming all voltage signals are in phase, the total radiated field should be the sum of the contributions from each trace. Figure 15 shows the envelope of the estimated worst-case radiation from the board at a distance of 3 m calculated using the voltage-driven radiation algorithm.

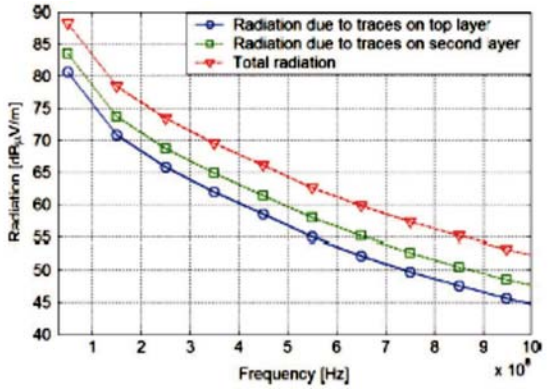

Fig.15. Radiation from the board calculated using the voltage-driven radiation algorithm.

The high frequency parametric and structural analysis of the Voltage-Driven Radiation Algorithm for the test board is illustrated in the figure 16 and 17.

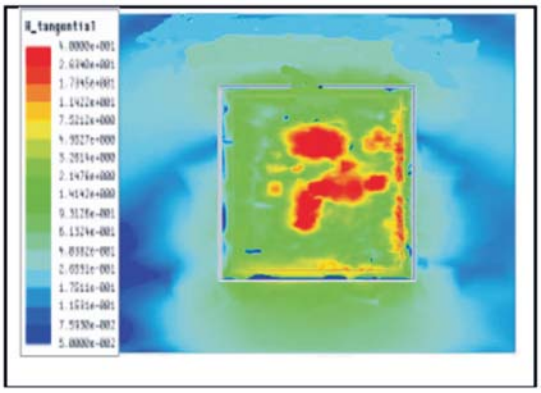

Fig. 16. High frequency parametric and structural analysis of the H-field in Voltage-Driven Radiation Algorithm

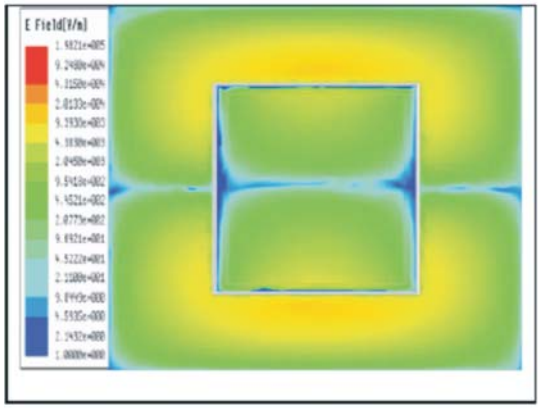

Fig. 17. High frequency parametric and structural analysis of the E-field in Voltage-Driven Radiation Algorithm

D. Board Analysis Using the Radiation by I/O coupling algorithm

High frequency signals can couple to input/output (I/O) nets that carry the coupled energy away from the board. The emission mechanism is illustrated in the figure 18. There are two primary high-frequency trace-to-trace coupling mechanisms, namely, capacitive and inductive coupling. Capacitive and inductive coupling are due to the electric and magnetic fields, respectively.

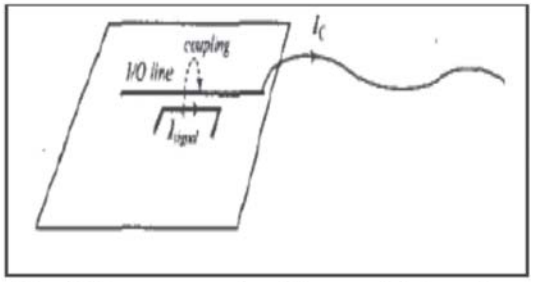

Fig. 18. Common-mode cable current induced by coupling to an I/O trace

The noise signal voltages induced on I/O lines due to capacitive and inductive coupling are given as,

$$V_{elec} = \omega C_m \times V_{signal} \times l_{eq} \times Z_{rec} \quad (11)$$

$$V_{mag} = \omega M \times I_{signal} \times l_{eq} \quad (12)$$

Where C_m is the mutual capacitance, M is the mutual inductance, V_{signal} is the voltage on the source segment, I_{signal} is the current on the source segment, l_{eq} – equivalent length of a parallel pair of segments and Z_{rec} is the impedance of the parallel combination of the source and load on the destination net.

But, only the maximum value (V_{mng} or V_{elec}) is stored as the noise voltage (V_N) used to estimate emissions. The total noise voltage driving an I/O net is calculated as the sum of the induced noise voltages on each segment of the IO net.

Considering an attached cable as an isotropic radiator, conservation of power implies that,

$$\oint\!\!\oint \frac{1}{2}\frac{|E|^2}{\eta_o} ds = 4\pi r^2 \left(\frac{1}{2}\right)\frac{|E|^2}{\eta_o} = \frac{1}{2} R_{rad} I_{CM}^2 \quad (13)$$

where η_0 - free-space wave impedance (=120 π Ω) and R_{rad} -input impedance of a lossless resonant wire antenna.

At low frequencies, it is more reasonable to calculate the radiated field for an electrically short antenna as,

$$R_{rad} = 80\pi^2 \left(\frac{l}{\lambda}\right)^2 = 80\pi^2 \left(\frac{f\,l}{c}\right)^2 \quad (14)$$

where, l is the length of an antenna and c is free-space wave velocity. This suggests that the length of cable can be modeled as 1 m with reasonable accuracy. The radiated field at low frequencies can be is estimated as,

$$E_{rad} = 3.4\times10^{-7} f\, I_{CM} \quad (15)$$

Equation (14) and (15) are approximately equal at 118 MHZ. Therefore, the radiated field due to the IO coupling mechanism is calculated by using equation (15) up to 118 MHz and equation (14) above 118 Mhz.

The total radiation at each frequency is calculated as the root mean square of the all the estimates, which is given by the equation,

$$|E|_{total} = [\sqrt{(E_{IO\ net\ 1})^2 + (E_{IO\ net\ 2})^2 \ldots (E_{IO\ net\ S})^2}] \quad (16)$$

The parameters needed to calculate the radiation by the differential mode radiation algorithm are listed in Table 4.

Table 4. Parameters needed Differential mode algorithm

Parameter	Description	Value
L	Board length	7.6 cm
W	Board width	5.0 cm
h	Space between power planes	0.05 mm
ε_r	Dielectric permittivity	3.88
R_s	Average resistance of the components	0.3 ohms
L_s	Average inductance of the components	1.4 nH
t_1	Rise/fall time of the current signal	1.5 ns
t_2	Rise/fall time of the current signal	1.5 ns
T	Period of the signal	20 ns
C_{PD}	Power dissipation capacitance	20 pF/gate

A large conducting patch at the lower side of the PCB is connected to the 9 V reference and surrounds all the six ICs. All the ground pins of the ICs are connected to the surrounded ground patch with the star-point pattern. Figure 19 shows the radiated emissions of the PCB. However, when the 30 cm wire is connected to the PCB ground, radiated emissions due to CM radiation mechanism increase substantially with some of these emissions exceeded the limit, as shown in figure 20. This indicates that by applying the wrong grounding concept will lead to surprising EMI results.

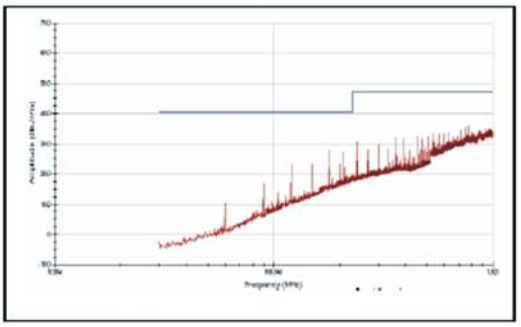

Fig. 19. Radiation by I/O coupling algorithm emissions for PCB layout

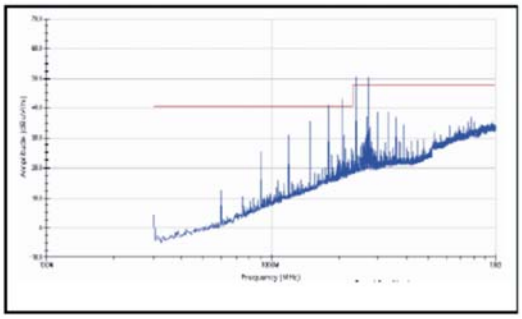

Fig. 20. Radiation by I/O coupling algorithm emissions for PCB with attached wire.

E. Board Analysis Using the Power Bus Radiation Algorithm

Transient currents drawn by the active devices on a PCB are a source of power bus noise. For high-speed digital systems, the resulting power bus voltage fluctuation cannot only lead to functional problems but also result in significant radiated emissions. The inductance associated with decoupling capacitors plays an important role at high frequencies. Figure 21 illustrates typical layouts for connecting a decoupling capacitor

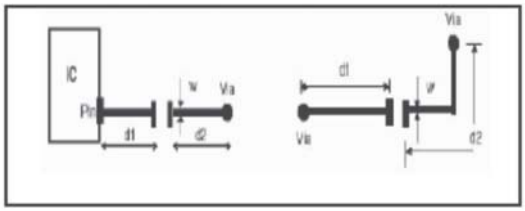

Fig. 21.Typical geometry of traces for connecting power bus decoupling capacitors .

The series inductance corresponding to the traces is calculated using the following equation 17.

$$L = 200 \times (d_1 + d_2) \times [2 + \ln(h/w)] + 1 \quad [nH] \qquad (17)$$

The effective capacitance of each decoupling capacitor changes with frequency due to the series inductance and is calculated as,

$$C_{eff,i} = \min\left(\left|C_i / (1 - \omega^2 L_i C_i)\right|,\ 2C_i\right) \qquad (18)$$

If the effective capacitance of a decoupling capacitor is much smaller than the inter-plane capacitance (i.e.Ceff,i<Co/10), then the capacitor is ignored and stored in a list of ineffective capacitors.

The power bus radiation algorithm computes the radiation coming directly from the power bus on a board with power planes. The maximum intensity of the radiated emissions from a rectangular power bus structure can be derived, based on an analytical cavity-resonator model. The effect of components mounted on the board is modeled by modifying the propagation constant of the waves within the power bus structure. The maximum radiated field intensity is given by

$$|E| = \frac{120I}{\varepsilon_r \min(L, W)} \frac{h}{r} Q(f) \qquad (19)$$

Where I is the current drawn from the power planes, L is the equivalent length of the power planes, W is the equivalent width and length of the power planes, h is the spacing between the plane pair, r is the distance from the board to the measurement point, is the Q(f) – resonance quality factor of the power bus structure.

The algorithm was first applied to the test board when the buffers were not loaded. The parameters needed to calculate the radiation by the power bus radiation algorithm and their values are listed in Table 5.

Table 5. Parameters needed for Power Bus algorithm

Parameter	Description	Value
L	Board length	7.6 cm
W	Board width	5.0 cm
h	Space between power planes	0.05 mm
ε_r	Dielectric permittivity	3.88
R_c	Average resistance of the components	0.3 ohms
L_c	Average inductance of the components	1.4 nH
t_1	Rise/fall time of the current signal	1.5 ns
t_2	Rise/fall time of the current signal	1.5 ns
T	Period of the signal	20 ns
C_{PD}	Power dissipation capacitance	20 pF/gate

Figure 21 shows the maximum radiation from structural analysis of the H-field in Power Bus the board calculated by the power bus Radiation Algorithm radiation algorithm. At low frequencies, the emissions are limited primarily by the component loss. Above 500 MHz, the radiation decreases primarily because the energy in the power bus current waveform decreases.

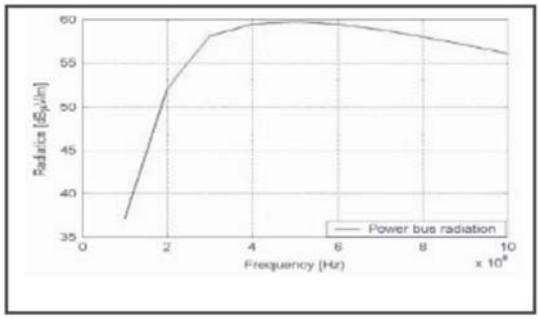

Fig. 21(a). Radiation from the board calculated using the power bus radiation algorithm.

The high frequency parametric and structural analysis of the Power Bus Radiation Algorithm for the test board is illustrated in the figure 22 and 23.

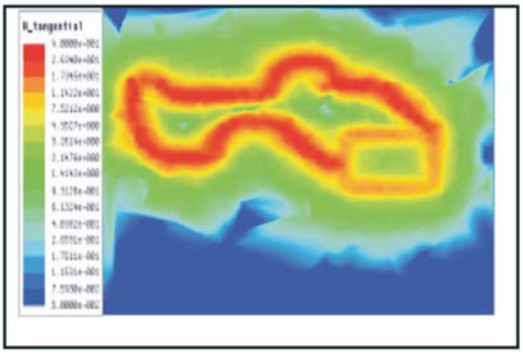

Fig. 22. High frequency parametric and structural analysis of the H-field in Power Bus Radiation Algorithm

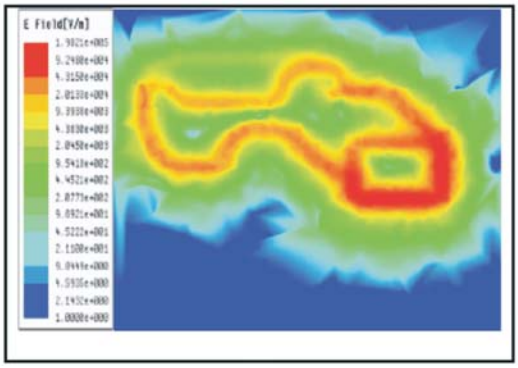

Fig. 23. High frequency parametric and structural analysis of the H-field in Power Bus Radiation Algorithm

VII. CONCLUSION

Although both of the layout problems identified by the EMC expert software system might have been obvious to an EMC engineer who was familiar with the board and the signals on each of these nets, a lot of effort would have been required to initially locate these problems manually. If changes were made to the layout, this effort would have to be repeated to ensure that no new problems were created. The expert system algorithms are designed to help both experts and non-experts find major potential problems early in the design process without manually examining every net routed on the board.

REFERENCES

[1] H. Shim, T. Hubing, T. Van Doren, R. DuBroff, J. Drewniak, D. Pommerenke, and R. Kaires, 2004, "Expert system algorithms for identifying radiated emission problems in printed circuit boards," in Proc. IEEE Int. Symp. Electromagn. Compat., Santa Clara, CA, vol. 1, pp. 57–62.

[2] H. Shim and T. Hubing, 2005, "Model for estimating radiated emissions from a printed circuit board with attached cables driven by voltage-driven sources," IEEE Trans. Electromagn. Compat., vol. 47, no. 4, pp. 899–907.

[3] H. Shim and T. Hubing, 2005, "Derivation of a closed-form approximate expression for the self-capacitance of a printed circuit board trace," IEEE Trans. Electromagn. Compat., vol. 47, no. 4, pp. 1004–1008.

[4] D. Hockanson, J. Drewniak, T. Hubing, F. Sha, and M. Wilhelm, 1996, "Investigation of fundamental EMI source mechanisms driving common-mode radiation from printed circuit boards with attached cables," IEEE Trans. Electromagn. Compat., vol. 38, no. 4, pp. 557–565.

[5] H. Shim, Y. Fu, and T. H. Hubing, 2004, "Radiated emissions from populated printed circuit boards due to power bus noise," in Proc. IEEE Int. Symp. Electromagn. Compat., Santa Clara, CA, vol. 2,Aug. 9–13, pp. 396– 400.

[6] H. Shim and T. Hubing, 2006, "A closed-form expression for estimating radiated emissions from the power planes in a populated printed circuit board," IEEE Trans. Electromagn. Compat., vol. 48, no. 1, pp. 74–8.

[7] F. Schnieder and W. Heinrich, 2001, "Model of thin-film microstrip line for circuit design," IEEE Trans.Microw. Theory Tech., vol. 49, no. 1, pp. 104– 110.

[8] M. Leone, 2003, "The radiation of a rectangular power-bus structure at multiple cavity-mode resonances," IEEE Trans. Electromagn. Compat., vol. 45, no. 3, pp. 486–492.

[9] J. Fan, W. Cui, J. L. Drewniak, T. P. Van Doren, and J. L. Knighten, 2002, "Estimating the noise mitigation effect of local decoupling in printed circuit boards," IEEE Trans. Adv. Packag., vol. 25, no. 2, pp. 154–165.

Pearson.T received B.E. and M.E. degrees in Electronics Engineering from Bharathiar University, Coimbatore, India. His research interests include the study of electromagnetic interference effects on CMOS digital circuits and digital circuits on VLSI systems particularly device modeling and circuit design.